A&A 438, 867–874 (2005)
DOI: 10.1051/0004-6361:20052820

Astronomy & Astrophysics

Cool carbon stars in the halo

II. A study of 25 new objects⋆,⋆⋆

N. Mauron[1], T. R. Kendall[2,⋆⋆⋆], and K. Gigoyan[3]

[1] Groupe d'Astrophysique, UMR 5024 CNRS, Case CC72, Place Bataillon, 34095 Montpellier Cedex 5, France
e-mail: mauron@graal.univ-montp2.fr
[2] Laboratoire d'Astrophysique, Observatoire de Grenoble, Université Joseph Fourier, BP 53, 38041 Grenoble Cedex 9, France
[3] 378433 Byurakan Astrophysical Observatory & Isaac Newton Institute of Chile, Armenian Branch, Ashtarak d-ct, Armenia

Received 4 February 2005 / Accepted 29 March 2005

Abstract. We present new results from an ongoing survey of carbon-rich asymptotic giant (AGB) stars in the halo of our Galaxy. After selecting candidates primarily through their 2MASS colours, slit spectroscopy was achieved at the ESO NTT telescope. Twenty-one new AGB carbon stars were discovered, increasing the total of presently known similar AGB C stars to ∼120. A further four were observed again in order to confirm their carbon-rich nature and measure radial velocities. Two main findings emerge from this work. First, we found a C star located at ≈130 kpc from the Sun and at $b = -62°$. This distant star is remarkably close (5 kpc) to the principal plane of the Stream of the Sagittarius dwarf galaxy, and is likely to be a tracer of a distant poorly populated southern warp of the Stream. Such a warp is predicted by model simulations, but it passes ∼45 kpc from that star. The second result is that, mainly in the North, several already known or newly discovered AGB carbon stars lie far, up to 60 kpc, from the mean plane of the Sagittarius Stream.

Key words. stars: carbon – Galaxy: halo – galaxies: stellar content

1. Introduction

This paper is a continuation of our previous paper devoted to cool, asymptotic giant branch (AGB), carbon (C) stars that are found at high galactic latitude or, alternatively, far from the galactic plane (Mauron et al. 2004, hereafter Paper I). Historically, these stars have attracted the attention of observers for several reasons: their characteristic observability due to the CN and C_2 bands in their spectra, their rarity (∼100 are presently known), and their high luminosity as AGB stars, which make them useful for studying the stellar content of the galactic halo at large distances (see for example Wallerstein & Knapp 1998; Totten & Irwin 1998, hereafter TI98). For illustration, in the I-band, Demers et al. (2003) found from the study of several Local Group galaxies that the average I-band absolute magnitude of (not too dusty) AGB C stars is $M_I = -4.6$. This average luminosity leads one to expect an apparent magnitude as bright as $I = 15.4$ for a distance of 100 kpc.

In the halo of the Galaxy, the majority, but not all, of the cool AGB C stars originate in the debris of the Sagittarius (Sgr) dwarf galaxy that orbits the Milky Way (Ibata et al. 2001; see also Paper I). One could also think that the Magellanic Stream might contain carbon stars, but no stellar population has been discovered in this stream despite many investigations, such as deep imagery with the Keck telescope (Guhathakurta & Reitzel 1998, and references therein).

The cool stars that we study here are different from, and rarer than, other types of C rich stars found with deep observations at high galactic latitude, e.g. the high velocity CH stars and other types of warm C rich metal poor giants, and the population of C rich dwarfs (for more details see e.g., Wallerstein & Knapp 1998; Margon et al. 2002; Downes et al. 2004). In this paper, we focus on the AGB-type stars, which are usually understood as originating in intermediate age populations. The important point that drives our work is that the census of these cool and luminous AGB C stars located out of the galactic plane is far from complete. Our goal is therefore to improve our knowledge of this population of halo C stars and to increase the number of these objects.

A first step towards achieving this task is to obtain a selection of candidates located at latitudes $|b| > 30°$ and faint enough

⋆ Based on observations made at the European Southern Observatory, Chile (program 73.A-0030), and on data from the 2MASS project (University of Massachusetts and IPAC/Caltech, USA).
⋆⋆ Appendix is only available in electronic form at http://www.edpsciences.org
⋆⋆⋆ *Present address*: Centre for Astrophysics Research, Science & Technology Research Institute, University of Hertforshire, College Lane, Hatfield AL10 9AB, UK.

Table 1. List of observed faint cool halo carbon stars. Coordinates α and δ (J2000) are given in the object names (2MASS Jhhmmss.ss±ddmmss.s). l, b are in degrees. The magnitudes B & R are from the USNO-A2.0 as given in the 2MASS catalogue, from the APM database (Irwin 2000) or from the USNO-B1.0 (Monet et al. 2003), with uncertainties of the order of 0.4 mag. The JHK_s values are from the 2MASS all-sky point source catalogue, with uncertainties of the order of 0.02–0.03 mag.

No.	2MASS name	l	b	B	R	$B-R$	J	H	K_s	$J-K_s$	Note
31	2MASS J001655.77 −440040.6	323.07	−71.74	17.6	14.1	3.5	9.821	8.381	7.074	2.747	new
32	2MASS J082915.12 +182307.2	206.23	+29.57	16.1	11.5	4.6	8.748	7.709	7.067	1.681	new
33	2MASS J082929.03 +104624.1	214.18	+26.61	19.3	13.0	6.3	10.260	9.008	8.138	2.122	new
34	2MASS J085418.70 −120054.0	239.10	+20.47	19.0	12.4	6.6	10.753	9.213	8.020	2.733	new
35	2MASS J085955.71 −775305.4	292.01	−20.27	20.1	14.3	5.8	12.865	11.557	10.554	2.311	new
36	2MASS J101037.00 −065113.9	248.12	+38.35	16.9	12.9	4.0	9.952	9.073	8.527	1.425	new
37	2MASS J114142.36 −334133.2	286.69	+26.97	18.5	16.3	2.0	13.848	12.802	12.178	1.670	Gizis
38	2MASS J121416.94 −090050.0	287.66	+52.75	18.4	15.3	3.1	13.222	12.355	11.875	1.347	new
39	2MASS J130953.60 +232541.0	352.37	+84.42	18.0	14.1	3.9	11.751	10.464	9.486	2.265	Lieb.
40	2MASS J131901.11 +042021.2	320.24	+66.28	19.0	15.7	3.3	13.074	12.245	11.847	1.227	new
41	2MASS J134723.04 −344723.3	315.77	+26.68	17.7	14.6	3.1	12.081	10.848	10.099	1.982	new
42	2MASS J143758.36 −041336.1	346.37	+49.44	17.3	14.5	2.8	12.265	11.411	10.903	1.362	new
43	2MASS J144631.08 −005500.2	352.23	+50.60	19.2	15.3	3.9	12.409	11.541	11.054	1.355	Marg.
44	2MASS J145726.98 +051603.4	2.52	+52.89	–	18.2	–	14.242	12.676	11.438	2.804	new
45	2MASS J152244.43 −123749.4	350.55	+35.89	19.2	15.5	3.7	13.080	11.983	11.433	1.647	new
46	2MASS J152723.59 +042827.8	8.58	+46.49	15.9	12.0	3.9	10.159	9.020	8.127	2.032	new
47	2MASS J165227.70 −160738.4	3.82	+17.31	19.7	16.2	3.5	13.138	12.107	11.525	1.613	Gizis
48	2MASS J184650.29 −561402.8	339.65	−21.66	18.9	15.5	3.4	12.714	11.683	11.038	1.676	new
49	2MASS J191424.18 −782241.5	316.01	−27.68	18.5	14.7	3.8	9.662	8.486	7.434	2.228	new
50	2MASS J193138.52 −300230.5	9.09	−21.27	19.5	14.5	5.0	11.970	10.931	10.289	1.681	new
51	2MASS J193709.84 −353014.9	03.88	−24.10	17.6	15.0	2.6	11.950	10.787	10.222	1.728	new
52	2MASS J193734.14 −353237.6	03.86	−24.20	–	15.0	–	11.266	10.001	9.125	2.141	new
53	2MASS J224350.35 −570123.3	331.15	−52.54	14.7	12.5	2.2	9.539	8.523	7.995	1.544	new
54	2MASS J224628.52 −272658.2	+24.98	−62.31	19.4	17.0	2.4	14.867	13.890	13.274	1.593	new
55	2MASS J224738.01 −782717.2	310.32	−36.83	16.7	12.9	3.8	10.023	8.907	8.214	1.809	new
	Three warm carbon stars: one from TI98, and two from Christlieb et al. survey										
56	2MASS J031424.48 +074443.99	172.87	−40.87	17.7	15.8	1.9	13.770	13.062	12.805	0.965	TI98
57	2MASS J211720.79 −055047.60	45.55	−34.95	16.5	15.4	1.8	12.472	11.786	11.615	0.857	Chris.
58	2MASS J211742.10 −065711.00	44.41	−35.56	16.6	14.8	1.9	12.673	12.000	11.808	0.865	Chris.

Notes: The last column (note) indicates whether the halo C star is a new discovery of this work or whether its C rich nature was already established in the literature (i.e. Gizis 2002; Liebert et al. 2000; Margon et al. 2002; TI98 = Totten & Irwin 1998; Christlieb et al. 2001).

to avoid members of the galactic disk. Subsequently, one has to provide confirmation with follow-up spectroscopy. This experiment related in Paper I showed that about one third of the candidates selected with 2MASS photometry and confirmed spectroscopically appear to be true AGB C stars. The task is more difficult when one wishes to explore regions at lower latitude, down to $|b| \sim 20°$, as we have attempted in this study, because contamination by young stellar objects with similarly red colours becomes greater. In the following, we describe new findings of C stars in the distant halo, and especially the discovery of a very distant C star at about 130 kpc from the Galactic Centre.

2. Selection of candidates

The selection method for cool halo AGB C stars has been described in Paper I. Here, we briefly recall it and mention some changes that have been made since Paper I. Carbon star candidates are now selected from the final, full-sky release of the 2MASS photometric catalogue[1]. Apart from a few exceptions, we impose limits $K_s < 13.5$, $J - K_s > 1.3$. The limit in K_s is sufficiently faint to allow detection of AGB C stars at large distances in the halo, and the colour limit is imposed to avoid increasing contamination of candidates by M type stars. $J - H$ and $H - K_s$ colours are requested from 2MASS such that the representative point in a JHK_s colour–colour diagram lies within 0.15 mag of the relatively narrow locus formed by the known cool C stars at high galactic latitude ($|b| > 30°$) (see Paper I). This narrow locus of C stars in the JHK_s diagram

[1] www.ipac.caltech.edu/2MASS

Table 2. Adopted template carbon stars used for deriving radial velocities by cross-correlation. Their velocities, noted v_{helio}, are in km s^{-1}.

Star	v_{helio}	Run
APM 1019−1136	+126 ± 4	April
APM 1406+0520	−21 ± 5	April
APM 1519−0614	+105 ± 4	April
IRAS 17446−7809	−5 ± 5	August
APM 2213−0017	−44 ± 3	August
APM 0207−0211	−140 ± 5	August

is seen well, for example, in Fig. 2 of Nikolaev & Weinberg (2000). Another change compared to Paper I is that we consider targets down to the latitude $|b| = 20°$, giving especially attention to candidates that are faint in K_s, that is, K_s typically greater than ∼8.0. This is done with the idea that, if the targets actually are AGB C stars, they are distant and far from the galactic plane, and do not belong to the common disk N-type C star population.

After 2MASS candidates are identified with the above photometric criteria, they are systematically checked in various catalogues with Simbad (CDS). They are also examined in POSS digitized surveys and when possible, on the objective prism plates of Byurakan Observatory (Gigoyan et al. 2001). Candidates already known as C stars are excluded, except for specific reasons such as measuring a missing radial velocity or improving uncertain cases observed previously. These various checks result in many candidates being discarded because they appear to be M-type giants, galaxies, QSOs, young stellar objects, T Tauri stars, M-type or even L-type dwarfs (e.g. Kendall et al. 2003). Some cases can also be eliminated as artefacts by inspecting the POSS and 2MASS images.

3. Observations

Two runs were carried out at the NTT telescope of ESO (Chile) during the nights Apr. 15–17, 2004 and Aug. 17–20, 2004. The instrument was EMMI used in the medium dispersion mode (REMD) with a slit of 1″ and grating "D/7". This grating has 600 g mm^{-1}, is blazed at 6000 Å, and is used with an OG 530 filter. The detector was an MIT-LL 2048×4096 CCD with 15×15 μm pixels used in 2×2 binning and normal readout mode. The resulting dispersion is 0.81 Å per pixel, and the resolution was $\lambda/\delta\lambda \sim 2600$ (corresponding to 115 km s^{-1}, or $\delta\lambda = 2.7$ Å at 7000 Å). The observed wavelength range was 6406–7940 Å for the first run and 6312–7890 Å for the second run, the difference being due to an error in instrumental setting. Each on-target exposure was followed immediately (without depointing the telescope) by a spectral calibration exposure made with a helium lamp (3 s) and an argon lamp (30 s). The exposure times on targets were from ∼10 to ∼60 min.

Because the radial velocities of the targets are obtained by cross-correlation, at least three C rich stars ("templates") with relatively well known radial velocities were observed each night (see Paper I and below). One photometric standard was also observed to perform an approximate flux calibration. Because the target objects are in general cool and variable; and since we ignore various photometric effects, e.g. slit losses and sky transparency, the absolute flux calibration can be only indicative, but the slope of the spectra could be interesting to consider in future work.

4. General properties of the observed stars

A total of 54 selected candidates were observed in the two ESO runs reported above. Among these 54 candidates were included three that were already suspected to be C rich by Gigoyan et al. (2002; 2003) but needed firm confirmation (objects #32, #33, and #46). From this sample, we obtained a total of 21 confirmed new AGB C stars as listed in Table 2. In this table, the running number follows the numbers of the stars described in Paper I.

This list from #31 to #55 also includes 4 stars which were known to be C rich with certainty but deserved more observations (objects #37, #39, #43, and #47). Objects #37 and #47 had been noted C-type in Tables 1 and 2 of Gizis (2002), who found them while searching for brown dwarfs in the TW Hya association, but no spectra and radial velocity were available for them. Note that object #47 has a low galactic latitude of $b = +17°$, and therefore was not included in our initial list of candidates, which is limited to $|b| > 20°$. Object #39 was discovered by Liebert et al. (2000), while #43 was discovered in the Sloan survey by Margon et al. (2002); and for both cases, a measurement of their heliocentric radial velocity $v_{\rm helio}$ was desirable.

Finally, in addition to this main sample, we included three stars here that were observed in previous runs, but not reported in Paper I. Of these 3 stars, #56 is an object listed in TI98 but without radial velocity, and the two others were selected from the ESO-Hamburg sample of Christlieb et al. (2001). All three objects have $J - K_s \sim 0.9$, which allowed us to compare the spectra of these warm objects to those having $J - K_s > 1.3$, which constitute our main sample.

In order to estimate the efficiency of our survey for finding new C stars, we do not consider those 4 stars that were already known to be C rich with certainty: 2 from Gizis, 1 from Liebert, 1 from Sloan. There remain 54 candidates, of which 21 were found to be new C stars. Our efficiency is therefore close to 39%, somewhat better than the observation efficiency reported in Paper I (30%).

Concerning the global properties of the 25 stars numbered #31 to #55, one can note that the R-band magnitude has a range of 11.5 to 18.2, whereas the $B - R$ colour index is, in most cases, larger than 3. Only 5 cases have $B - R < 3$. Two objects have no $B - R$: object #44 has no B available because of its extreme faintness, and its $J - K = 2.8$ confirms that this object is very cool and possibly dusty. For #52, no reliable B and R data are available in catalogues because of blending. We tentatively estimated its R magnitude through a comparison to star #51, which lies on the same digitized POSS2 red plate and is separated by only ∼5.5′ from #52. A similar estimation was attempted for the B-band, but its quality was too poor to be considered.

In the 2MASS data (K_s, $J - K_s$) of the same sample #31 to #55, one can note first that K_s lies largely in the range 7.0 to 12.2, with a median of 10.1 identical to the K_s-band median of the C stars discovered in Paper I. In the list presented here, there is, however, a remarkably faint object, #54, with $K_s = 13.27$. This source will be discussed below in more detail.

The colour index $J - K_s$ of our sample lies in the range 1.3 to 2.8, with one exception for object #40 with $J - K_s = 1.227$. This last object was found in a tentative selection where we sought candidates having $1.2 < J - K_s < 1.4$ with added constraints $K_s > 11$ and $B - R > 3$. Thus, our sample (#31 to #55) is made of carbon stars that are red, with $J - K$ larger than 1.2. This indicates that these stars cannot be early R-type stars, because early R-type objects have $J - K$ between 0.4 and 1.2, as can be derived from Table 1 in Knapp et al. (2001).

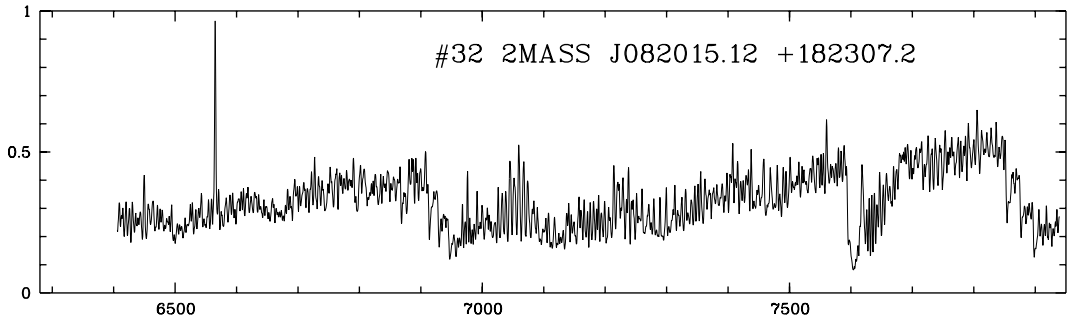

Fig. 1. A typical spectrum, here for object #32. The abscissa is wavelength in angstroms, and the ordinate is flux in erg s^{-1} cm^{-2} Å^{-1}, after division by an appropriate factor of 1.8×10^{-13}. The spectrum is dominated by CN and C_2 features, and Hα is in emission. The strong absorption band near 7600–7700 Å is telluric O_2. All other spectra are available in the electronic Appendix.

5. Spectra

For clarity, the complete atlas of all spectra is given in the electronic appendix, but for illustration the spectrum of #32, which is typical, is displayed here (Fig. 1). The spectra of the 25 objects #31 to #55 are very similar to those of Paper I with rising flux distributions. Of these 25 cases, 11 clearly show Hα in emission (like #32), a proportion of ∼45% of cases, exactly as the sample of Paper I. The last 3 objects #56, #57, and #58 are bluer in $J - K_s$ (≈0.9) and have a noticeably flatter continuum. Two clearly display Hα in absorption. In all spectra, the strong band at 7600–7700 Å is from telluric O_2.

6. Radial velocities

The radial velocities were determined by cross-correlating our program stars with at least three "template" stars of roughly the same apparent brightness, observed the same night and with previously determined velocities. These templates were chosen in Table 4 of TI98. A supplementary one, IRAS 17446-7809, was taken from the list of Loup et al. (1993). This star is also known as USNO-B1.0 0118-1022651 and its R-band magnitude is ∼11−12. Uncertainties on the velocities of these templates are indicated in Table 2, as given by TI98 for APM objects or estimated using the CO profile of Nyman et al. (2000) for IRAS 17446-7809. Consistency between the velocities of these templates was checked to be very good (<10 km s^{-1}) when correlating them one to one.

Beside these templates, we also re-observed APM 0915 − 0327, for which TI98 had given +79 km s^{-1}, whereas Mauron et al. (2004) had found +95 km s^{-1}. With our current data, all independent correlations with the other templates provide $v_{\rm helio} = +106$ km s^{-1} (±10 km s^{-1}). The spectra showed nothing peculiar, and we eventually rejected this star as a radial velocity template.

Erratum: in Paper I, an error was made for star #15, alias 2MASS J172825.76+700829.9. Its heliocentric radial velocity is −158 and not +158 km s^{-1}.

7. Proper motions

Information on proper motions from the USNO-B1.0 catalogue of Monet et al. (2003) is available for all the objects, except one: #51 which is blended with neighbours. For 19 objects, the USNO-B1.0 proper motion is zero, while for 8 objects, a non-zero proper motion is provided in USNO-B1.0 and listed in Table 3. One can see that these proper motions are very small in general, apart from the case of #58. In Paper I, we found the same situation with a few objects having very small but non-zero motions. The conclusion of those detailed investigations was that these very small proper motions were suspect, and probably artefacts. Essentially the same analysis could be done here.

Table 3. Data from the USNO-B1.0 database for objects with non-zero proper motions. N is the number of detections on the scanned plates, and Probab. is the total motion probability.

Object #	$\mu_\alpha \cos\delta$ (mas yr^{-1})	μ_δ (mas yr^{-1})	N	Probab.
36	+8 ± 3	+2 ± 6	5	0.8
44	−2 ± 0	−2 ± 0	3	0.8
45	+6 ± 2	+0 ± 6	4	0.9
47	−2 ± 3	+10 ± 1	4	0.9
53	−12 ± 0	+6 ± 8	4	0.9
55	−8 ± 15	+16 ± 2	4	0.9
57	−4 ± 5	+10 ± 2	5	0.8
58	+50 ± 13	−28 ± 10	4	0.9

In addition, an analysis of USNO-B1 data can be done by considering the reduced proper motion $H = J + 5\log_{10}(\mu)$. In Fig. 2, we have plotted H as a function of the color index $R - J$. The circles represent confirmed dwarf carbon stars with available 2MASS data belonging to the sample of Downes et al. (2004) or Lowrance et al. (2003). The filled squares represent the 16 C stars that we found in Paper I and in this paper, and for which the USNO-B1.0 proper motions are not zero, but suspect. One can see that, with the exception of one object (#58 at $R - J \approx 2.1$, $H \approx 6.5$), the locus of our C stars is very different from that of known dCs. This shows that, even if the proper motions were correct, there would be no dwarfs in our sample of cool ($J - K \geq 1.2$) C stars.

We shall hereafter ignore these proper motions when they are small. The case of #58 for which a proper motion of 57 mas yr^{-1} is relatively well measured will be treated in the next section.

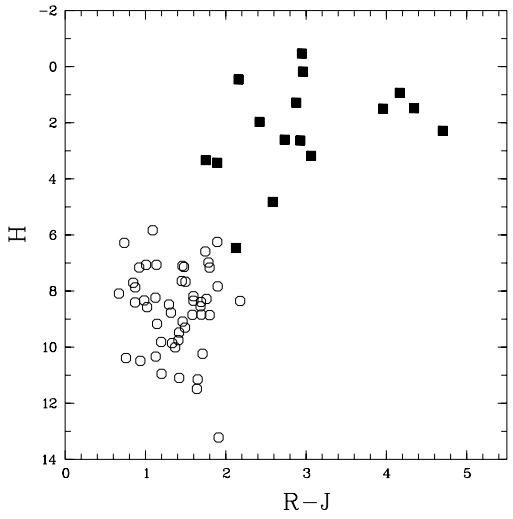

Fig. 2. The reduced proper motion $H = J + 5\log_{10}(\mu)$ plotted as a function of the $R-J$ color index. Open circles are known dwarf carbon stars. Filled squares represent the 16 C stars of our sample for which USNO-B1 provides a non-zero proper motion (see text).

8. Distances

Determination of distances was performed in the same way as in Paper I and is based on the $J - K_s$ and K_s data. The K_s-band absolute magnitude that was used is in turn based on the K_s magnitudes of C stars in the Large Magellanic Cloud (averaged in different bins in $J - K_s$) *plus* 0.5 mag, where this supplementary term is due to the average difference between C stars in the LMC and C stars in the Sgr dwarf galaxy (see Paper I for more details). The effect of interstellar reddening $E(B - V)$ is in general small but was taken into account, because several stars lie at at relatively low galactic latitude. The relations between $E(B - V)$ and the extinction in J and K_s were taken from the 2MASS documentation, i.e. its extinction calculator (Schlegel et al. 1998). We adopted $E(J - K) = 0.537\,E(B - V)$ and $A_K = 0.367\,E(B - V)$, and obtained the results listed in Table 2.

The intrinsic $(J - K_s)_0$ of the 3 last warm stars of Table 1 can be obtained after correction of reddening, and one finds $(J - K_s)_0$ between 0.76 and 0.80. This index suggests that they might be *early* R-type giants, but certainly not *late* R-type giants. For instance, this $J - K_s$ value is bluer by at least 0.3 mag than all the $J - K_s$ values of the late R-type sample of Knapp et al. (2001), who found that the K_s-band absolute magnitude of early R-type giants is on the order of -2.0 ± 1, and that the early R-type stars are clump giants.

If we adopt the view that all three stars are clump giants, i.e. with $M_{K_s} \sim -2$, then their distances are found to be 8.6, 5.1, and 5.6 kpc for #56, #57, and #58, respectively. This, however, cannot be true for #58, because such a luminosity would imply an unfeasibly large transverse velocity, v_t. Since $v_t(\mathrm{km\,s^{-1}}) = 4.75\,\mu(\mathrm{mas\,yr^{-1}}) \times d(\mathrm{kpc})$, one would find $v_t \sim 1500\,\mathrm{km\,s^{-1}}$, far too great for a star in our Galaxy. Therefore, significantly lower luminosity than that of a clump giant is necessarily implied, and #58 is a dwarf carbon (dC) star, provided the USNO-B1.0 data are correct. Its K_s absolute magnitude might be on the order of ∼+7 (Lowrance et al. 2003). Then one finds $d \sim 90$ pc and $v_t \sim 25\,\mathrm{km\,s^{-1}}$, consistent with the radial velocity of $70\,\mathrm{km\,s^{-1}}$. An additional indication that #58 is a dwarf is the presence of strong absorption NaI lines, which are not seen in the spectra of the two other stars for which the NaI lines were observed (#56 and #57).

9. Analysis and discussion

When the sample of cool C stars investigated above (#31 to #55) is added to previous similar cases (Paper I, TI98), one obtains a total of 119 stars; therefore, it is interesting to geometrically represent this population of C stars in the halo. In the two panels of Fig. 3, we plotted all known halo AGB C stars in the galactocentric system. In this system, the Sun is at $X_\odot = -8.5$ kpc, $Y_\odot = Z_\odot = 0$. The Z axis is toward the North galactic pole and the Y axis is towards the longitude $l = +90°$. Note that the X coordinate is the one chosen by Newberg et al. (2003) or Bellazzini et al. (2002), but the opposite of that used in some other works. In our coordinates, the Sagittarius dwarf galaxy is at $X_{Sgr} = +14.6$ kpc, $Y_{Sgr} = +2.3$ kpc, and $Z_{Sgr} = -5.8$ kpc. The C stars discovered in this paper are indicated by crosses, while those discovered in previous works are indicated by circles. Criteria to be included in these two plots were that the objects have $J - K_s > 1.2$, in order to select only AGB stars, and $|Z| > 1.5$ kpc, in order to eliminate C stars which are almost certainly members of the galactic disk.

For comparison to the data, in Fig. 4 we plotted the N-body simulation of the Sgr Stream given by Law et al. (2004) [2]. We chose to show the simulation for a spheroidal Galactic potential, since it is a compromise between the oblate and prolate cases, each of which have advantages and disadvantages, as discussed by Law et al. (2004). We emphasize that our goal here is not to further improve this model, which already includes as many as 11 geometric and velocity constraints based on detailed studies of the Sgr dwarf and its Stream (see Law et al., their Sect. 2). Rather, we intend to focus on the question of where the C stars are located and what this tells us, despite their scarcity and the relative uncertainty of their distances on the order of ±15% (1σ) for a given $J-K_s$ (see Paper I).

In Fig. 3, the left-hand diagram shows that the large majority of C stars lie along a slightly inclined but roughly South/North straight line, which is the plane of the Sgr Stream seen nearly edge-on (see, e.g., the upper panels of Fig. 7 in Majewski et al. 2003), and this is also in fair agreement with the left-hand panel of Fig. 4. The extension in Z of the main cloud of points, ignoring the outliers, i.e. from $Z \sim -40$ to $Z \sim +45$ kpc, is similar in the observations and in the model, giving credence to the C star distance scale adopted here and in Paper I.

One particular object that we discovered is #54 = 2MASS J224628.52−272658.2. It is the object plotted as a cross with the lowest Z in Fig. 3, left panel. Its distance to the Sun, based on the use of its K_s and $J-K_s$ values, is $d \approx 130$ kpc with $Z \approx -118$ kpc, $Y \approx +26$ kpc, and $X \approx +47$ kpc. If our distance scale is correct, this star #54 appears as the most

[2] http://www.astro.virginia.edu/~srm4n/Sgr/

Table 4. Properties of the halo C stars. Quantities l, b, R, K_s, $J-K_s$ are repeated from Table 2 for information. The colour excess $E(B-V)$ is taken from the maps of Schlegel et al. (1998), in magnitudes, with uncertainty of the order of 0.01 mag. The quantity M_{K_s} is the K_s-band absolute magnitude derived for each object, and is used to derive the distance to the Sun, d, in kpc. Uncertainties (1σ) on M_{K_s} and d are ∼0.3 mag and 15%, respectively. Z is the height above or below the galactic plane, in kpc. The measured heliocentric velocity $v_{\rm helio}$ is in km s^{-1}, with uncertainty of the order of ∼10 km s^{-1} (1σ). The last column is the same as in Table 1.

No.	l	b	R	K_s	$J-K_s$	$E(B-V)$	M_{K_s}	d	Z	$v_{\rm helio}$	Note
31	323.07	−71.74	14.1	7.074	2.747	0.007	−7.25	7.5	−7.0	−38	new
32	206.23	+29.57	11.5	7.067	1.681	0.032	−7.45	8.0	4.0	+111	new
33	214.18	+26.61	13.0	8.138	2.122	0.035	−7.55	13.5	6.0	+90	new
34	239.10	+20.47	12.4	8.020	2.733	0.049	−7.30	11.5	4.0	+130	new
35	292.01	−20.27	14.3	10.554	2.311	0.192	−7.45	39.0	−13.5	+270	new
36	248.12	+38.35	12.9	8.527	1.425	0.035	−7.10	13.0	8.0	+306	new
37	286.69	+26.97	16.3	12.178	1.670	0.071	−7.40	82.0	37.0	+144	Gizis
38	287.66	+52.75	15.3	11.875	1.347	0.045	−6.95	58.0	46.0	+106	new
39	352.37	+84.42	14.1	9.486	2.265	0.013	−7.45	24.5	24.0	+57	Lieb.
40	320.24	+66.28	15.7	11.847	1.227	0.030	−6.65	50.0	45.0	+49	new
41	315.77	+26.68	14.6	10.099	1.982	0.066	−7.65	35.0	15.5	+139	new
42	346.37	+49.44	14.5	10.903	1.362	0.101	−6.90	36.0	27.0	+102	new
43	352.23	+50.60	15.3	11.054	1.355	0.043	−7.00	40.0	31.0	+54	Marg.
44	2.52	+52.89	18.2	11.438	2.804	0.040	−7.25	55.0	44.0	−13	new
45	350.55	+35.89	15.5	11.433	1.647	0.162	−7.35	55.0	32.0	+126	new
46	8.58	+46.49	12.0	8.127	2.032	0.052	−7.60	14.0	10.0	+134	new
47	3.82	+17.31	16.2	11.525	1.613	0.738	−6.65	38.0	11.0	+117	Gizis
48	339.65	−21.66	15.5	11.038	1.676	0.083	−7.40	49.0	−18.0	+75	new
49	316.01	−27.68	14.7	7.434	2.228	0.220	−7.55	9.5	−4.5	+177	new
50	9.09	−21.27	14.5	10.289	1.681	0.121	−7.40	34.0	−12.0	+128	new
51	03.88	−24.10	15.0	10.222	1.728	0.290	−7.35	31.0	−13.0	+137	new
52	03.86	−24.20	15.0	9.125	2.141	0.288	−7.60	21.0	−7.5	+153	new
53	331.15	−52.54	12.5	7.995	1.544	0.017	−7.30	11.5	−9.0	+131	new
54	24.98	−62.31	17.0	13.274	1.593	0.022	−7.35	130.0	−120	+2	new
55	310.32	−36.83	12.9	8.214	1.809	0.152	−7.55	14.0	−8.5	+378	new
				Three warm carbon stars							
56	172.87	−40.87	15.8	12.805	0.965	0.317	−2.0	8.5	−5.5	−155	TI98
57	45.55	−34.95	15.4	11.615	0.857	0.180	−2.0	5.0	−3.0	−151	Chris.
58	44.41	−35.56	14.8	11.808	0.865	0.131	+7.0	0.1	−0.06	−70	Chris.

distant *cool* C star in the halo, more distant than any of the TI98 C stars. We note here that this star has a zero proper motion in the USNO-B1.0 catalogue, supporting the case for a bona-fide distant AGB C star.

The existence in the halo of similar distant objects is important. It is possible that other very distant *warm* C stars may be contained in the Sloan sample of Downes et al. (2004). More precisely, the Downes sample contains 20 objects for which the proper motions are lower than 5 mas yr^{-1}, that is, essentially undetected, and for which no classification as dwarf (D) is given (they are marked U in their Table 1). The same authors also found three certain members of the Draco dwarf galaxy, which is at a distance of 79 kpc (van den Bergh 2000). The average of their Sloan r magnitudes is $r \approx 17.0$, which provides an approximate distance scale ($M_r = -2.5$). Of the 20 stars mentioned above, 9 have $r > 19$ and some of them, if not dwarfs, may be more distant than 200 kpc. In summary, #54 might not be the only case of a C star at more than 100 kpc, but attributing a definite giant type (rather than dwarf) to the stars of Downes et al. is currently not possible.

Star #54 has another peculiarity: it is almost in the plane of the Sgr Stream. More precisely, adopting the Newberg et al. (2003) formulation and XYZ coordinates described above, this plane is defined as:

$$-0.064\,X + 0.970\,Y + 0.233\,Z = 0.232 \quad (1)$$

and it is readily found that object #54 is only 5 kpc from this plane; this distance to the plane is called $d_{\rm plane}$ hereafter. This shift is remarkably small given its large distance (∼130 kpc) to the Galactic Centre.

One can note in Fig. 4 that the Stream only extends as far as 100 kpc to the Southern Galactic regions. Also, the agreement is rather poor in the XZ panel of Fig. 4, that is, no Sgr debris particles are present close to #54, with about 40 kpc between #54 and the closest points shown in Fig. 4. This may suggest that we overestimate the distance of #54 *provided* we choose to trust the model points. Additional discoveries of C stars, or RGB stars, with comparable distances, radial velocities, and galactic latitudes ($b < -60°$) would be most useful to clarify this point.

At the upper part of the left panel in Fig. 3, one sees several stars which are off the mean Sgr Stream plane mentioned above. Distances to the Stream plane can exceed 20 kpc and are as large as 60 kpc for one object with

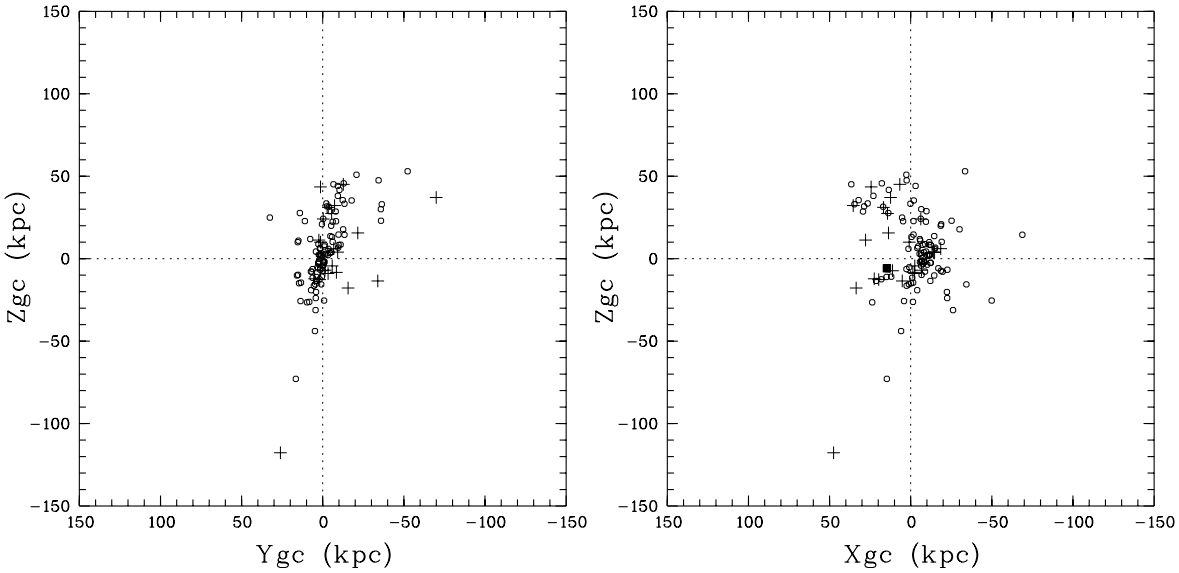

Fig. 3. Plots in galactocentric *XYZ* of the observed AGB C halo stars, with those found in this paper indicated by a cross. *Left panel*: the C stars trace the Sgr Stream seen nearly edge-on, with a very distant C star to the South, and several C stars off the plane in the North. *Right panel*: the Sun is at $X = +8.5$ kpc, $Z = 0$ to the right of the origin, and the Sgr dwarf galaxy centre is indicated by a filled square at $X = 14.7$ kpc $Z = -5.8$ kpc to the left of the origin. In the right panel, the scarcity of objects near the horizontal axis is due to the difficulty of finding very distant C stars close to the Galactic plane (see text).

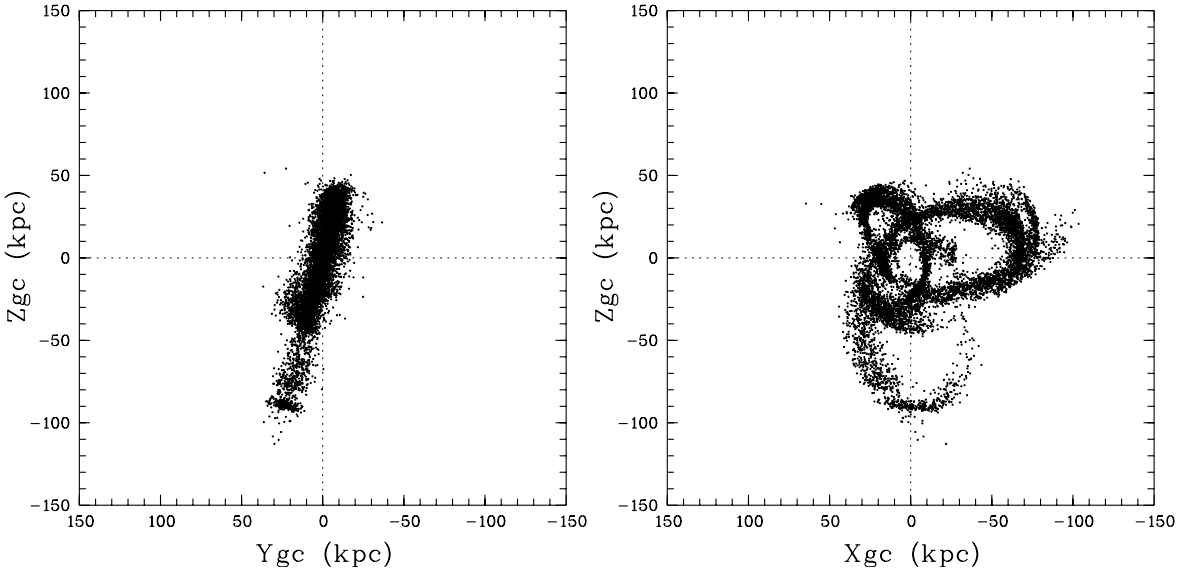

Fig. 4. Same plots in *XYZ* of the model of the Sgr Stream, from the *N*-body simulations of Law et al. (2004). This simulation corresponds to the case of a spheroidal Galactic potential.

$X = +12$ kpc, $Y = -70$ kpc, $Z = +37$ kpc. This object is our #37 = 2MASS J114142.36−334133.2 (found by Gizis 2002). Its distance to the Sun is 82 kpc, and this star has no sign of a proper motion in the USNO-B1.0 catalogue. Its colours are typical of an AGB C star.

There are 3 other objects for which the distance $d_{\rm plane}$ to the Stream mean plane exceeds 30 kpc. One is #35 from this paper ($d = 39$ kpc, $d_{\rm plane} = 36$ kpc), and another is #4 from Paper I ($d = 78$ kpc, $d_{\rm plane} = 36$ kpc). The last one is a faint high latitude variable star J1714.9+4210 studied by Meusinger & Brunzendorf (2004), also mentioned in TI98 and Kurtanitze & Nikolashvili (2000). It is also 2MASS J171457.52+421023.4. Meusinger & Brunzendorf (2004) found that this object is variable and has a C rich spectrum. We verified that its 2MASS colours are typical of a C star, located exactly on the narrow locus of the AGB carbon stars in the $JHK_{\rm s}$ diagram. Its has $K_{\rm s} = 11.17$ and $J-K_{\rm s} = 1.354$, $d = 43$ kpc, and $d_{\rm plane} = 37$ kpc. None of these four stars have any measurable proper motion. In summary, we have found 4 stars with typical AGB characteristics that are located between 30 and 60 kpc from the plane of the Stream. In addition, if we request $|d_{\rm plane}| > 20$ kpc, we get 9 stars, with only 1 on the left side in Fig. 3, the left panel (the Meusinger & Brunzendorf object), and 8 on the right side. This asymmetry is clearly visible in Fig. 3 (left panel) and does not seem to be predicted by the model.

The right panel of Fig. 3 is very different from what the model shows in the right panel of Fig. 4. Observations show in *XZ* that C stars are scattered within about 50 kpc from the

galactic centre with a few exceptions beyond this limit, while the model displays much larger extensions to the right and to the South of the centre. However, one has to take a number of observational limitations into account. In Fig. 3, right panel, the clump to the right of the centre is due to stars close to the Sun, and their numbers reflect the fact that they were more easily discovered than those located far away from the Sun. Another fact to take into account in interpreting the data is a lack of points near the $Z = 0$ plane. This directly reflects the presence of the galactic plane, which surveys for halo C stars naturally avoid. As a consequence, very few confirmed C stars can be seen near the core of the Sgr dwarf Galaxy, to the left of the figure centre, indicated with coordinates at $X_{\rm Sgr} = +14.6$ kpc and $Z_{\rm Sgr} = -5.8$ kpc.

Despite these difficulties in interpreting the *XZ* panel, we note an encouraging point of agreement: the observations indicate many C stars in the region delineated by *X* between 0 to +35 kpc and *Z* between +30 and +50 kpc. This region is ∼40 kpc above the Sgr dwarf centre (i.e. toward the North Galactic pole from Sgr) and the numerical models show that this region is abundant in the leading tidal debris of the Stream (see also Figs. 1 and 13 of Law et al. 2004).

10. Concluding remarks

From this second paper on the rare cool AGB C stars located in the Galactic halo, the main results are the following. We first discovered and/or documented 25 new cool C stars yielded by colour selection from the 2MASS photometric catalogue, and included new data for a few serendipitous discoveries previously reported in the literature. These stars have a distance $|Z|$ away from the galactic plane larger than ∼3 kpc and up to ∼130 kpc and cannot be ordinary N-type stars of the galactic disk.

We then considered the totality of all AGB C stars known in the halo (119 objects), and focused on their locations in the galactocentric *XYZ* system. Then, we compared them with one of the available *N*-body simulations of the Stream of the Sagittarius dwarf galaxy.

The majority of these cool C stars originate in the tidal disruption of the Sgr dwarf. A few remarkable objects deserve further study. For example, we discovered a very distant (∼130 kpc) southern C star, which is almost exactly in the mean plane of the Sgr Stream and more distant than any similar object hitherto documented. We also found four other remarkable C stars that are located off this plane, by large shifts, from 30 kpc to 60 kpc. None of these 4 objects seem to be dwarfs when 2MASS colours, spectra, proper motions, and other properties are considered. For a distance off the plane larger than 20 kpc, 9 stars were found.

Because cool AGB C stars are rare, observations of much more numerous (but fainter) red giants lying on the RGB are certainly needed to make our findings concerning the Sgr Stream geometry more robust. In some sense, the C stars can be considered as the reddest and most luminous tracers of a debris which remains to be found with deeper exploration. In the future, it will be interesting to see whether a systematic spectroscopic survey of our fainter candidates($R \sim 17$–21, ∼80 objects) would result in the discovery of more of these AGB C stars very far away in the halo, i.e. at distances from 100 to ∼200 kpc.

Acknowledgements. We would like to thank our referee, G. Wallerstein, for many comments that improved the manuscript. We acknowledge the use of the Two Micron All Sky Survey (2MASS), which is a joint project of the Univ. of Massachusetts and the Infrared Processing and Analysis Centre/California Institute of Technology, funded by NASA and NSF. This work also benefited from using the CDS database of Strasbourg. We also used the POSS-UKST Digitized Sky Survey made available by the Canadian Astronomical Data Centre and by the ESO/ST-ECF Centre in Garching. We also acknowledge the use of the MIDAS software of ESO with which all data processing and graphs were achieved.

References

Bellazzini, M., Ferraro, F., & Ibata, R. 2002, AJ, 125, 188
Christlieb, N., Green, P. J., Wisotzki, L., & Reimers, D. 2001, A&A, 375, 366
Demers, S., Battinelli, P., & Letarte, B. 2003, A&A, 410, 795
Downes, R. A., Margon, B., Anderson, S. F., et al. 2004, AJ, 127, 2338
Gigoyan, K., Mauron, N., Azzopardi, M., Muratorio, G., & Abrahamyan, H. V. 2001, A&A, 371, 560
Gigoyan, K. S., Abrahamyan, H. V., Azzopardi, M., & Russeil, D. 2002, Astrophys., 45, 322
Gigoyan, K. S., Abrahamyan, H. V., Azzopardi, M., et al. 2003, Astrophys., 46, 475
Gizis, J. E. 2002, ApJ, 575,484
Guhathakurta, P., & Reitzel, D. B. 1998, in Galactic Halos: a UC Santa Cruz Workshop, ed. D. Zaritsky, ASP Conf. Ser., 136, 22
Ibata, R. A., Lewis, G. F., Irwin, M. J., Totten, E., & Quinn, T. 2001, ApJ, 551, 294
Irwin, M. J. 2000, The APM Catalogue (the Web site is `http://www.ast.cam.ac.uk/~apmcat/`)
Kendall, T. R., Mauron, N., Azzopardi, M., & Gigoyan, K. 2003, A&A, 403, 929
Knapp, G. R., Pourbaix, D., & Jorissen, A. 2001, A&A, 371, 222
Kurtanidze, O. M., & Nikolashvili, M. G. 2000, in The Carbon Star Phenomenon, ed. R. Wing, IAU Symp., 177, 554
Law, D. R., Johnston, K. V., & Majewski, S. R., 2004, ApJ, 619, 807
Liebert, J., Cutri, R. M., Nelson, B., et al. 2000, PASP, 112, 1315
Loup, C., Forveille, T., Omont, A., & Paul, J. F. 1993, A&AS, 99, 291
Lowrance, P. J., Kirkpatrick, J. D., Reid, I. N., Cruz, K. L., & Liebert, J. 2003, ApJ, 584, L95
Majewski, S. R., Skrutskie, M. F., Weinberg, M. D., & Ostheimer, J. C. 2003, ApJ, 599, 1082
Margon, B., Anderson, S. F., Harris, H. C., et al. 2002, AJ, 124, 1651
Mauron, N., Azzopardi, M., Gigoyan, K., & Kendall, T. R. 2004, A&A, 418,77
Meusinger, H., & Brunzendorf, J. 2001, IBVS, 5035
Monet, D. G., Levine, S. E., Canzian, B., et al. 2003, AJ, 125, 984
Newberg, H. D., Yanny, B., Grebel, E. K., et al. 2003, ApJ, 596, L191
Nikolaev, S., & Weinberg, M. D. 2000, ApJ, 542, 804
Nyman, L. Ä., Booth, R. S., Carlström, U., et al. 1991, A&AS, 93, 121
Schlegel, D. J., Finkbeiner, D. P., & Davis, M. 1998, ApJ, 500, 525 (the IPAC extinction Web calculator site is `www.ipac.caltech.edu/forms/calculator.html`)
Totten, E. J., & Irwin, M. J. 1998, MNRAS, 294, 1 (TI98)
van den Bergh, S. 2000, The Galaxies of The Local Group (Cambridge University Press)
Wallerstein, G., & Knapp, G. R. 1998, ARA&A, 36, 369

Online Material

Appendix A: Spectra

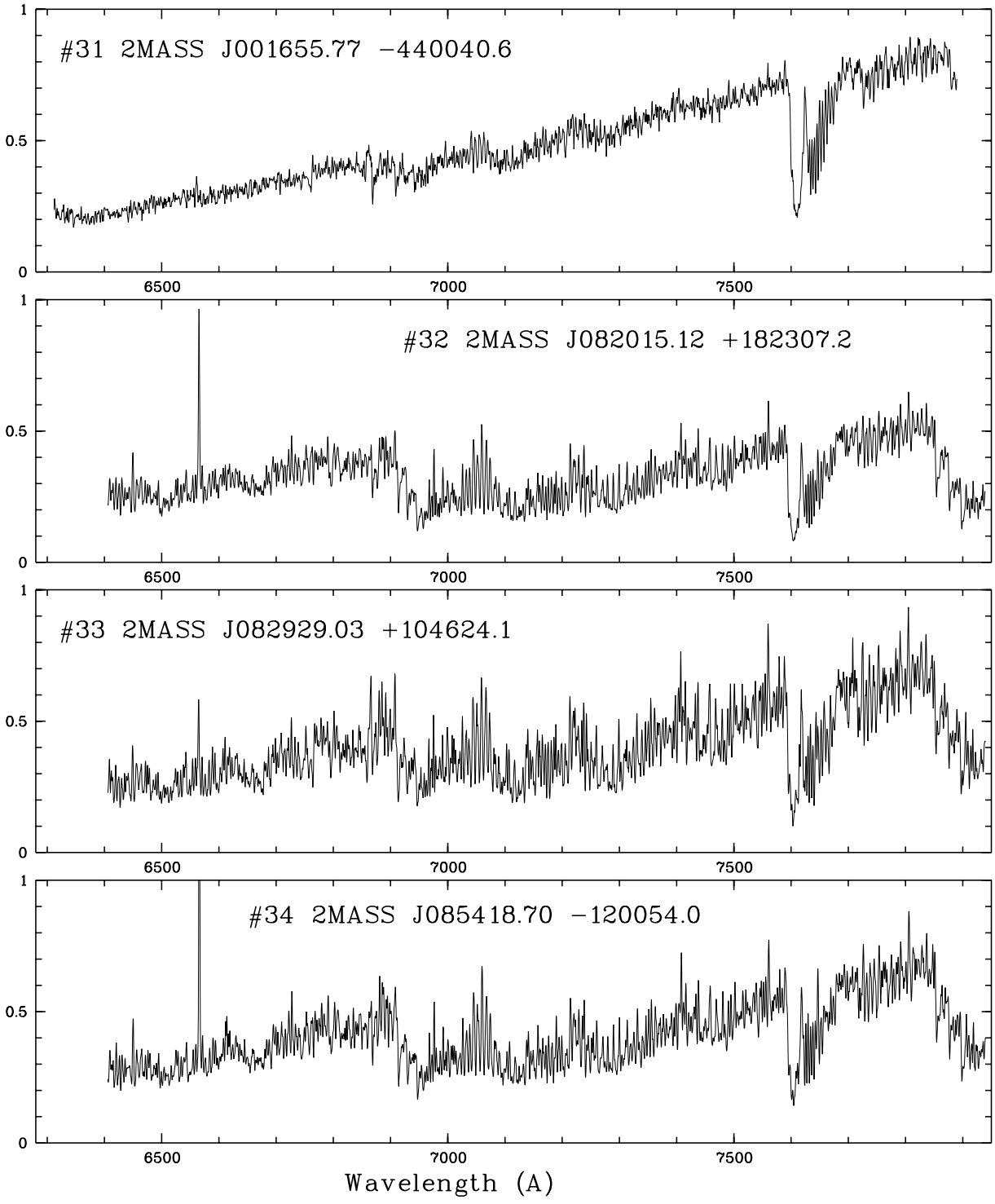

Fig. A.1. Spectra of objects 31, 32, 33, & 34. In all these graphs, fluxes in ordinates are in erg s^{-1} cm^{-2} Å^{-1}. Fluxes were divided by factors 0.7×10^{-14}, 1.8×10^{-13}, 0.5×10^{-13}, and 0.25×10^{-13} for objects 31, 32, 33, and 34, respectively.

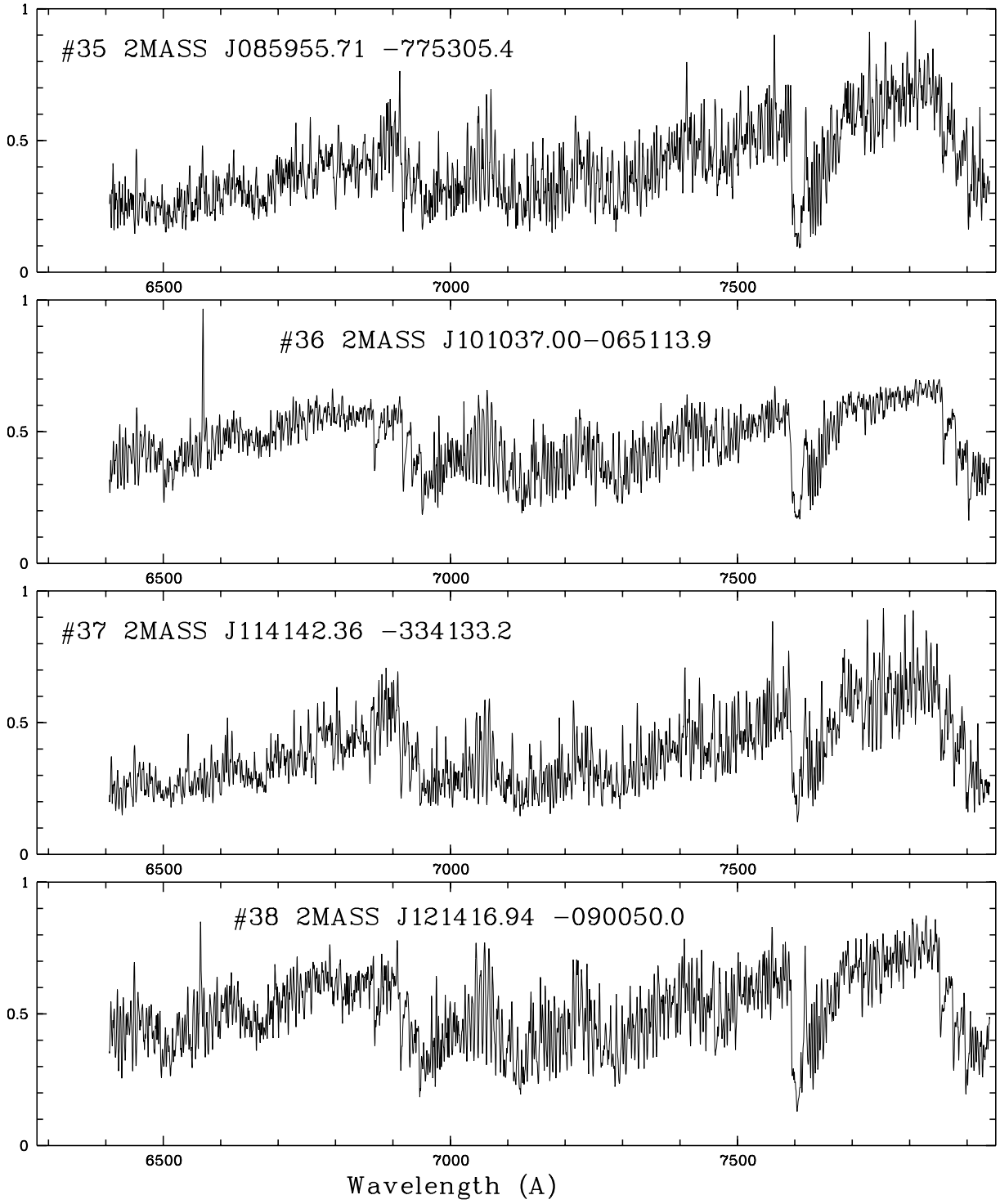

Fig. A.2. Spectra of objects 35, 36, 37, and 38. In all these graphs, fluxes in ordinates are in erg s^{-1} cm^{-2} Å^{-1}. Fluxes were divided by factors 0.18×10^{-14}, 5.5×10^{-15}, 0.22×10^{-14}, and 0.25×10^{-14} for objects 35, 36, 37, and 38, respectively.

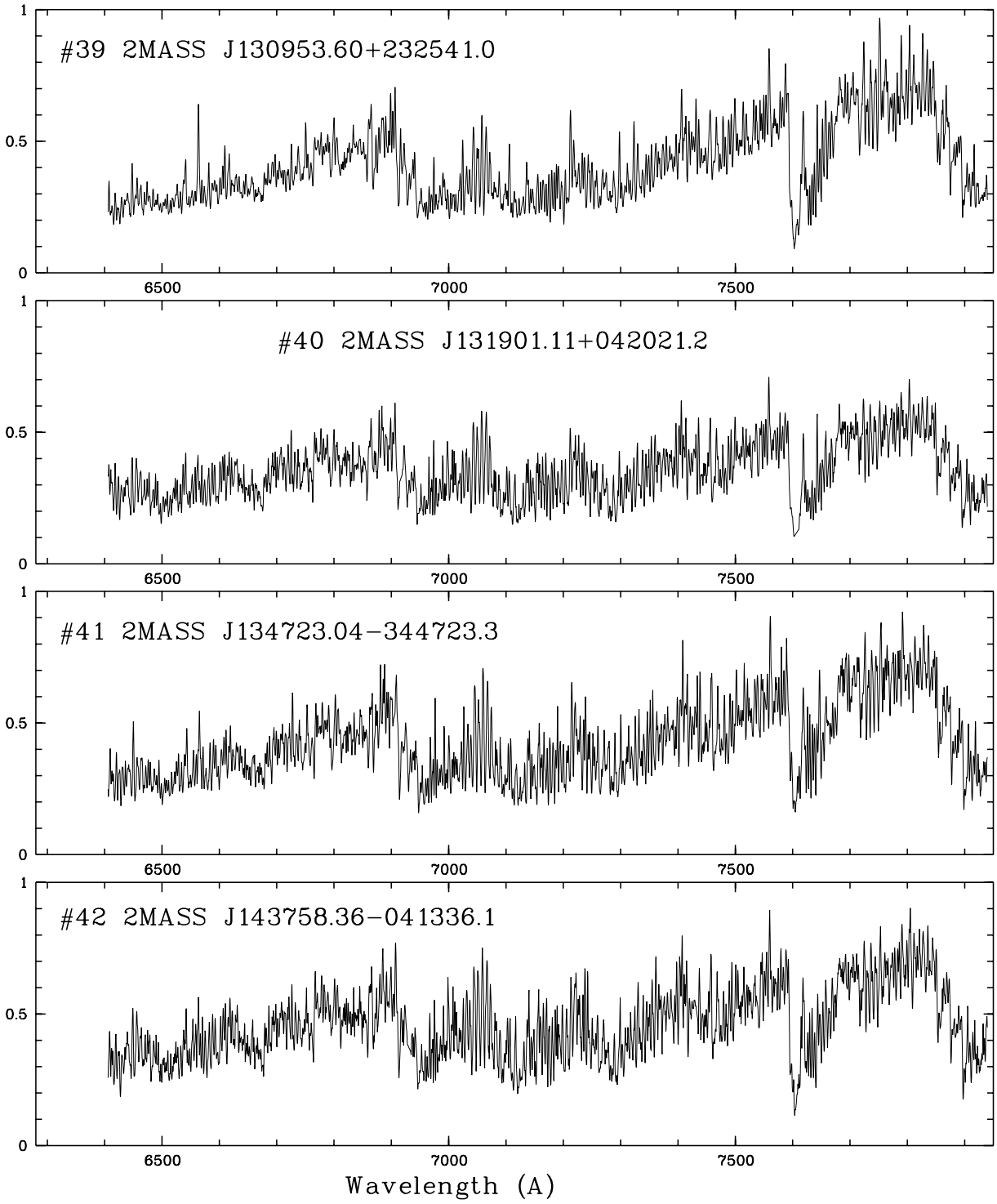

Fig. A.3. Spectra of objects 39, 40, 41, and 42. In all these graphs, fluxes in ordinates are in erg s^{-1} cm^{-2} Å^{-1}. Fluxes were divided by factors 0.95×10^{-14}, 3.5×10^{-15}, 0.9×10^{-14}, & 0.4×10^{-14} for objects 39, 40, 41, and 42, respectively.

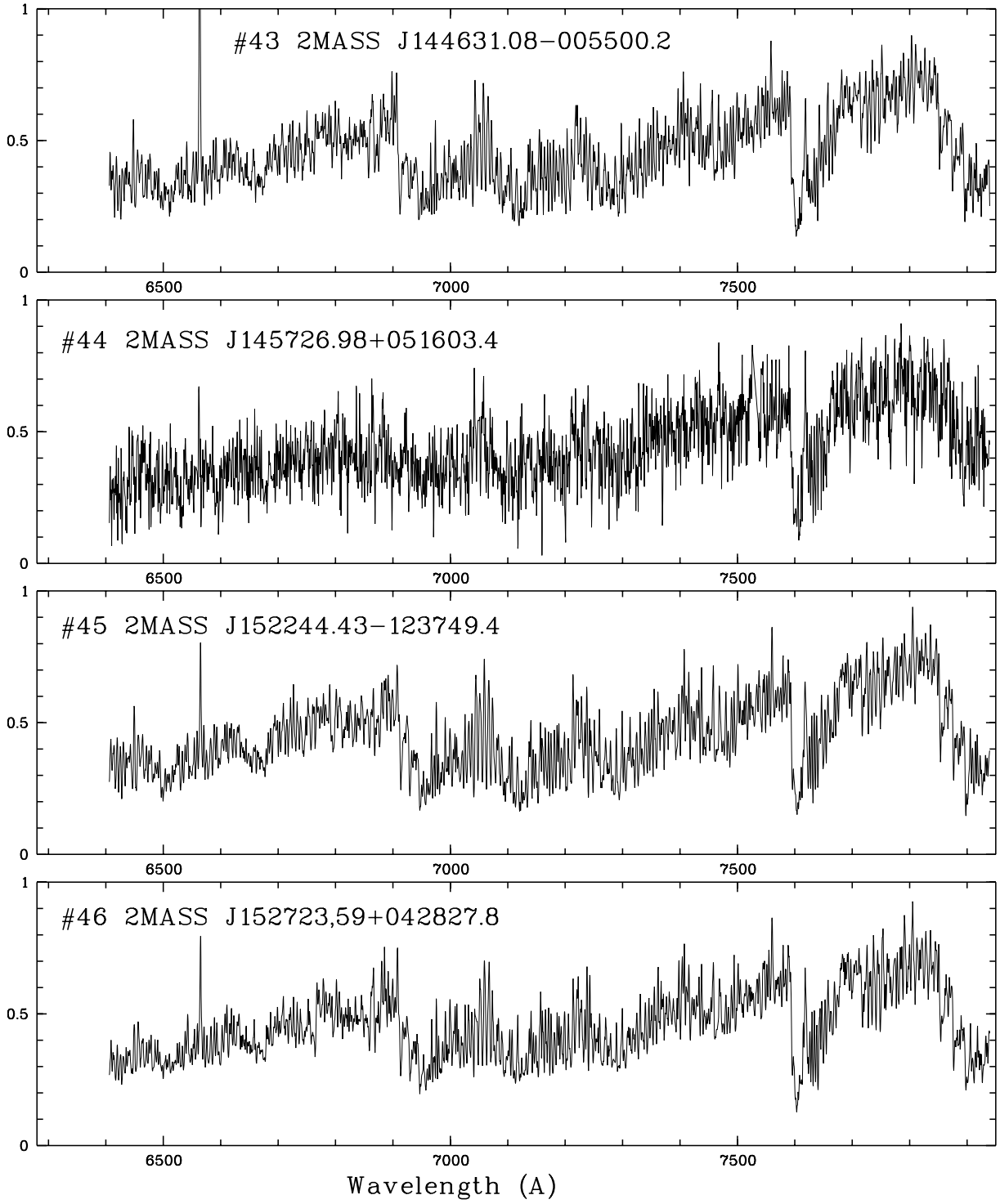

Fig. A.4. Spectra of objects 43, 44, 45, and 46. In all these graphs, fluxes in ordinates are in erg s^{-1} cm^{-2} Å^{-1}. Fluxes were divided by factors 0.22×10^{-14}, 0.017×10^{-14}, 4.5×10^{-15}, and 3.5×10^{-14} for objects 43, 44, 45, and 46, respectively.

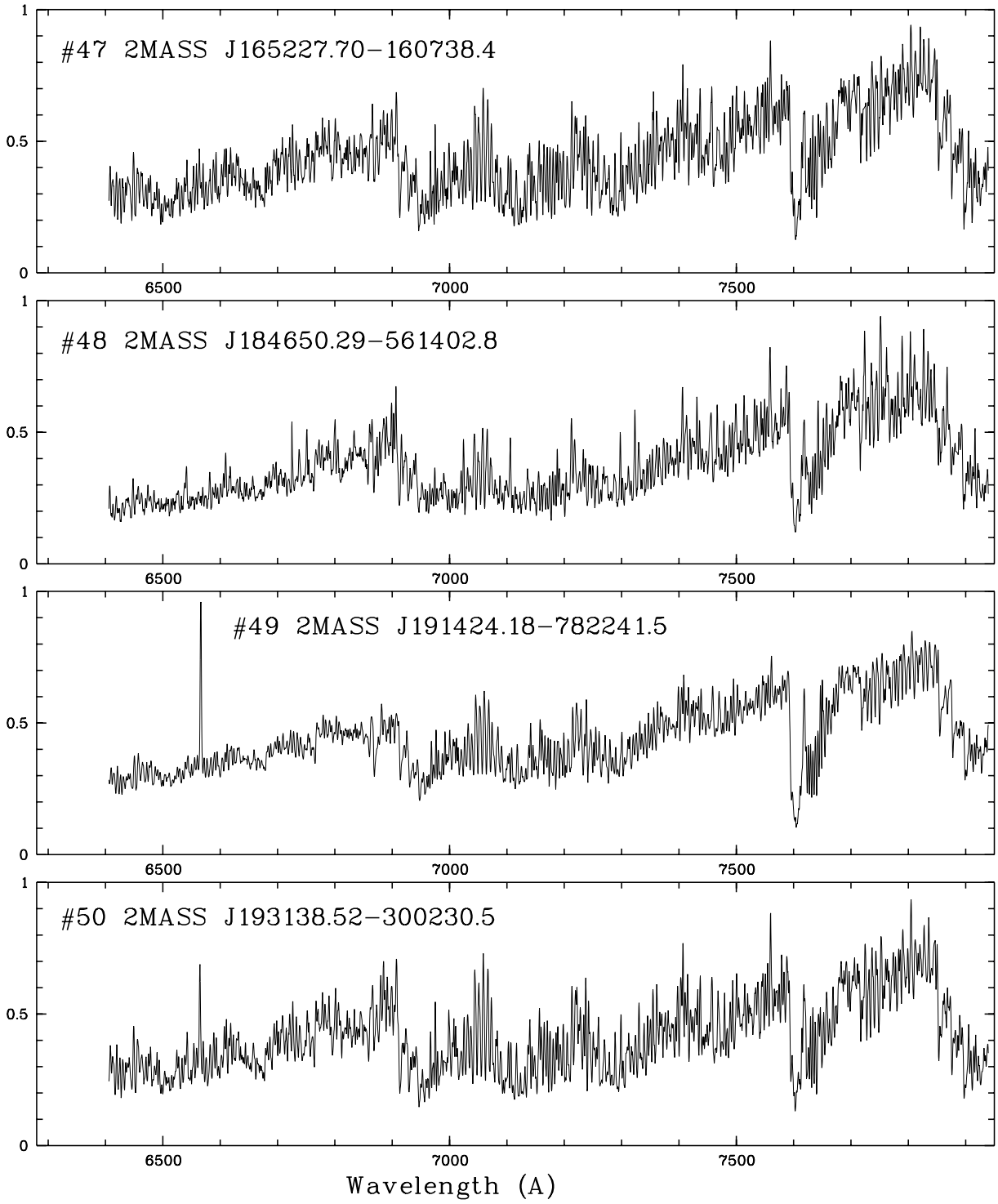

Fig. A.5. Spectra of objects 47, 48, 49, and 50. In all these graphs, fluxes in ordinates are in erg s^{-1} cm^{-2} Å^{-1}. Fluxes were divided by factors 0.15×10^{-14}, 2.6×10^{-15}, 3.3×10^{-14}, and 0.75×10^{-14} for objects 47, 48, 49, and 50, respectively.

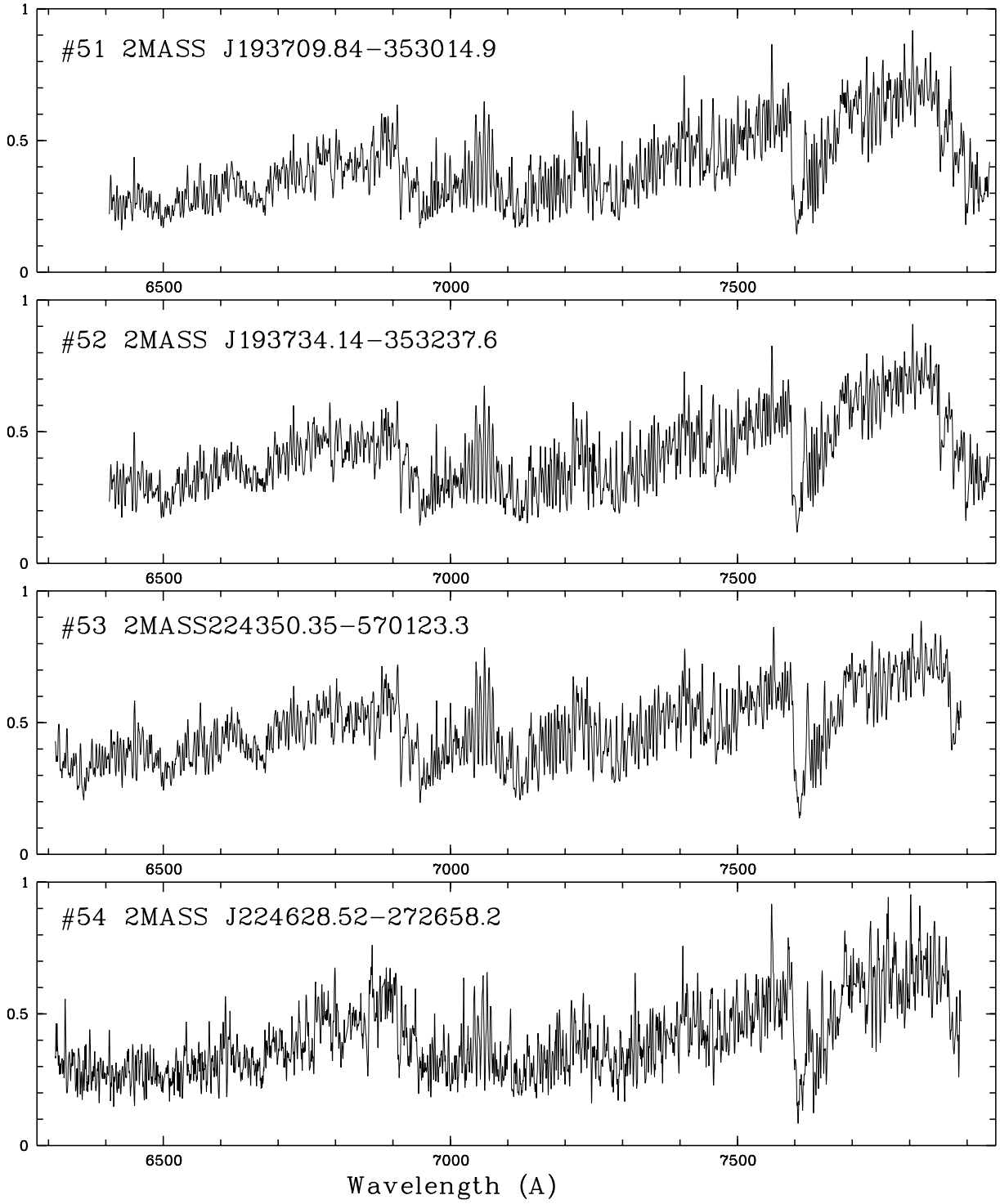

Fig. A.6. Spectra of objects 51, 52, 53, and 54. In all these graphs, fluxes in ordinates are in erg s^{-1} cm^{-2} Å^{-1}. Fluxes were divided by factors 0.6×10^{-14}, 2.7×10^{-14}, 5.5×10^{-14}, and 0.72×10^{-15} for objects 51, 52, 53, and 54, respectively.

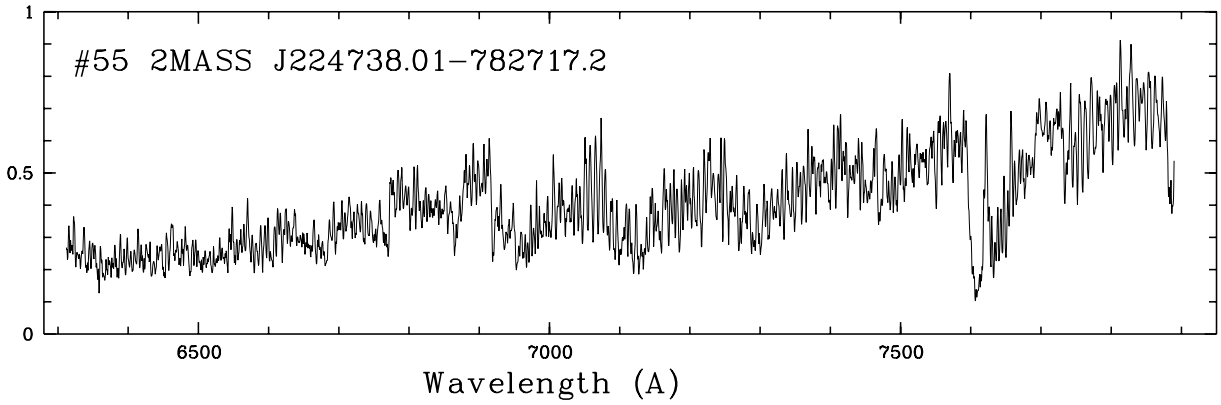

Fig. A.7. Spectrum of object 55. The flux in ordinates is in erg s^{-1} cm^{-2} Å^{-1}, after dividing by a factor of 2.2×10^{-14}.

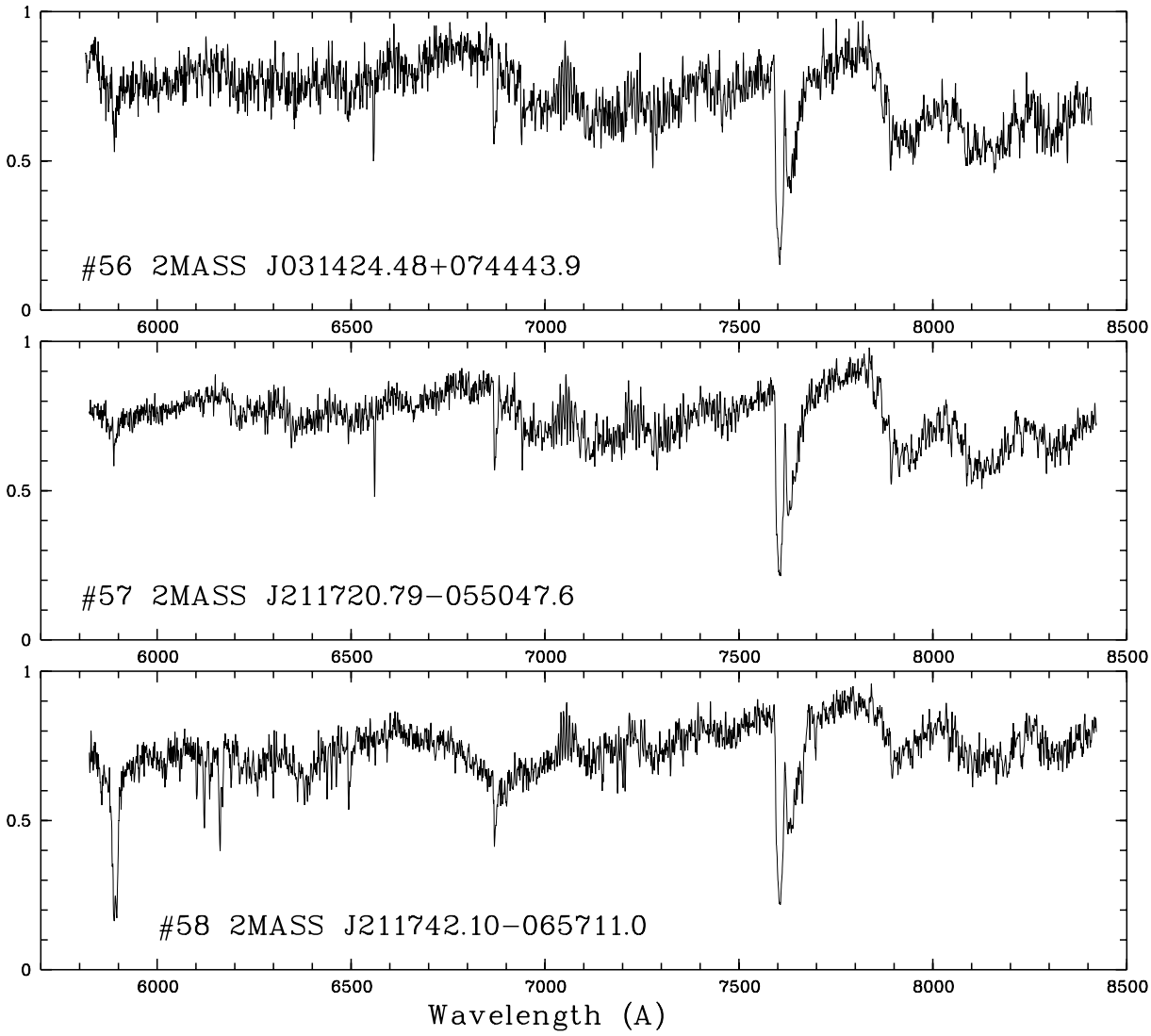

Fig. A.8. Spectra of objects 56, 57, and 58. In all these graphs, fluxes in ordinates are in erg s^{-1} cm^{-2} Å^{-1}. Fluxes were divided by factors 0.21×10^{-14}, 0.52×10^{-14}, and 3.7×10^{-15} for objects 56, 57, and 58, respectively.